4.70 (d, 1 H), 5.4 (s, 2 H), 5.75 (d, 1 H), 6.78 (d, 1 H), 7.30 (m, 5 H).

N-[α-Methylbenzyl]-1-propyl-2,4-dimethyl-1,4-dihydronicotinamide was prepared from the α-methylbenzylamine (Aldrich) and the 2,4-dimethylnicotyl chloride hydrochloride followed by alkylation and reduction according to the literature procedure,[7a] mp 119–120 °C dec (lit.[7a] mp 119.5 °C dec): NMR ($CDCl_3$) δ 0.90 (t, 3 H), 1.05 (d, 3 H), 1.45 (m, 2 H), 1.55 (d, 3 H), 2.05 (s, 3 H), 3.1 (t, 2 H), 3.25 (d, 1 H), 4.75 (d, 1 H), 5.25 (m, 1 H), 5.65 (s, 1 H), 5.75 (d, 1 H), 7.30 (m, 5 H).

General Procedure for Determination of the Kinetics of Reduction of *N*-Methylacridinium Iodide. Acetonitrile solutions containing either 0.015 mmol of *N*-methylacridinium iodide or 0.3 mmol of 1,4-dihydronicotinamide were deoxygenated by bubbling argon through each solution protected from the atmosphere with a septum. After the solution was deoxygenated the concentration of each solution was readjusted by the syringe addition of a few drops of acetonitrile. An aliquot of the 1,4-dihydronicotinamide solution (10^{-3}–2×10^{-2}) and an aliquot of the acridinium salt (10^{-3}) (with or without additives) were transferred by syringe to the two compartments of the stop–flow apparatus. Upon mixing at 19 °C the reactions were monitored for >5 half-lives (10–3000 s); see Table II).

A Hi-Tech stop–flow accessory (Hi-Tech Scientific Limited) was used to mix the two solutions. As a general procedure the decrease in the concentration of *N*-methylacridinium iodide was monitored by observing the decrease in the intensity of absorption at 420 nm ($\epsilon = 3620$); a constant infinity value was observed after a period between 1 and 12 h.

The UV spectrometer used is a HP 8450A diode array spectrophotometer connected to a HP 7470A plotter and a HP 82901M flexible disc drive.

General Procedure for the Reduction of α,α,α-Trifluoroacetophenone. An aliquot solution of DHNA (0.10 M), the ketone (0.050 M), and the additive was placed in a Pyrex reaction ampule, degassed, and sealed under vacuum. The ampule was thermostated in the dark in an oil bath at 61 °C for 96 h. The ampule was opened and an aliquot solution of the internal standard (0.04 M) was added. The product mixture was analyzed by GLPC using a 20 ft × $^1/_4$ in. glass column packed with 5% OV-101 on Chromosorb WAW DMCS, 100/120 mesh.

GLPC analyses were carried out on an HP 5840A gas chromatograph interfaced to a HP 5840A integrator. The area ratios were converted to mole ratios for quantitative determinations by using standard calibration curves constructed from known mixtures.

Products were identified by a comparison of their retention times, GLPC–mass spectra, and GLPC–IR and ^1H NMR spectra with those of authentic samples. Duplicate experiments were run with each ketone.

Cyclic Voltammetry. Electrochemistry was performed on a Princeton Applied Research EG & G Parc Model 175 universal programmer wave form generator equipped with a Amel Model 551 potentiostat that provided feedback compensation for ohmic drop between the working and reference electrodes. Voltammograms were recorded on a Tektronix 2430 digital oscilloscope equipped with a Hewlett-Packard Thinkjet printer. Electrochemical measurements were carried out at 25 °C in an anhydrous acetonitrile solution containing 5×10^{-3} M TFA and 0.1 M tetrabutylammonium perchlorate on a hanging mercury drop electrode. The voltammograms show a wave ($E_{1/2} = -1.69$ V vs $Ag/AgClO_4$, 10^{-3} M) which is completely reversible at sweep rates >1 V/s. A second irreversible wave at more negative potential is observed.

Acknowledgment. We thank the Natural Sciences and Engineering Research Council of Canada and the University of Alberta for their generous support of this work.

On the Relationship between Proximity and Reactivity. An ab Initio Study of the Flexibility of the $OH^\bullet + CH_4$ Hydrogen Abstraction Transition State and a Force-Field Model for the Transition States of Intramolecular Hydrogen Abstractions

Andrea E. Dorigo and K. N. Houk*

Department of Chemistry and Biochemistry, University of California—Los Angeles, Los Angeles, California 90024

Received September 10, 1987

Ab initio transition structures with various distance and angular constraints have been located for the hydrogen abstraction from methane by the hydroxyl radical. Some exemplary results are as follows: (1) when the CO distance in the transition state is constrained to be 0.1 Å longer than optimum, the predicted activation energy increases by 1.2 kcal/mol, which corresponds to a sevenfold decrease in rate at 25 °C; (2) a 20° change in the C···H···O angle from the optimum increases the activation energy by only 1 kcal/mol, which would result in only a sixfold decrease in rate. A force field has been developed to model the transition states of hydrogen abstraction by alkoxy radicals. Allinger's MM2 force field has been modified to incorporate force constants for atoms involved in bonding changes. Relative activation energies are calculated for intramolecular hydrogen abstractions by a variety of alkoxy radicals. The results agree with the experimental data which are available, and predictions of relative rate constants have been made for these and related reactions. The results also show that there is no simple relationship between calculated reaction rates and distances between the reacting atoms in the starting materials. The force-field model and ab initio calculations show that the preference for six-membered transition states over seven-membered is a result of a large entropic preference for the six-membered transition structure.

Introduction

There has been intense interest in the relationship between the proximity of reacting centers and the rate of reaction.[1-6] This issue is of particular importance for understanding how enzymes catalyze bimolecular reactions with astonishing efficiency. Prompted by a recent stimulating review of the subject by Menger,[7] we have undertaken theoretical studies[8] which we believe will lead

(1) Storm, D. R.; Koshland, D. E., Jr. *J. Am. Chem. Soc.* **1972**, *94*, 5815.
(2) Bruice, T. C.; Brown, A.; Harris, D. O. *Proc. Natl. Acad. Sci. U.S.A.* **1971**, *68*, 658.
(3) Delisi, C.; Crothers, D. M. *Biopolymers* **1973**, *12*, 1689.
(4) Page, M. I.; Jencks, W. P. *Proc. Natl. Acad. Sci. U.S.A.* **1971**, *68*, 1678.
(5) Page, M. I. *Angew. Chem., Int. Ed. Engl.* **1977**, *16*, 449.
(6) Jencks, W. P. *Adv. Enzymol. Relat. Areas Mol. Biol.* **1975**, *43*, 219.
(7) Menger, F. M. *Acc. Chem. Res.* **1985**, *18*, 128.

0022-3263/88/1953-1650$01.50/0 © 1988 American Chemical Society

eventually to a more thorough understanding of the detailed mechanisms of enzyme catalysis. Our initial studies have been designed to understand intramolecular reactivity in simple cases in which the geometries of reacting centers are fairly well-defined. In this paper, we describe the investigation of the rate of intramolecular hydrogen abstraction by alkoxy radicals. This reaction has been extensively studied mechanistically[9] and has been applied successfully in natural product synthesis,[10] particularly in the field of steroids.[11]

In his recent account,[7] Menger postulates that the reactivity in a series of structurally similar compounds should depend primarily upon the distance between the reacting functional groups, and the time that these functionalities spend at an optimal distance. Our computational study[8] of the lactonization of a variety of hydroxy acids has shown that this postulate fails to predict relative reactivities, at least for that reaction. We believe that, in general, rate constants cannot be accounted for only on the basis of a few parameters such as the distance between reacting atoms in the starting material and the time spent nearby and that quantitative predictions can only be based on a quantitative evaluation of the energies of reactants and transition states. The force field which we have developed for the modeling of lactonization transition states enables us to calculate relative activation energies for different compounds. The relative rate constants derived from these calculated barriers are in good agreement with the experimental values.[8]

One of our objectives in developing a model for the reactions described in the present paper was to determine the sensitivity of the reaction rate to constrained distortions away from ideal distance and angles. For the latter purpose it was necessary to study a model reaction which would be simple enough to allow a detailed ab initio MO theory study but would also be closely related to the intramolecular reaction that we had chosen to investigate. The hydrogen atom abstraction from methane by the hydroxyl radical satisfies both requirements. The transition state for this reaction had been located previously by Pople,[12] using the 6-31G** basis set[13] and electron correlation energy corrections with second-order Møller–Plesset perturbation theory.[14] Since we were interested in determining how the transition-state energy would be affected by changes in the geometry, we have investigated the same reaction using the smaller 3-21G[13] basis set and Hartree–Fock theory. We have made use of the Gaussian 82[15] program developed by Pople and co-workers for all calculations. We have calculated the energy and geometry of the transition state at this level of theory, as well as the energy of a number of "quasi-transition states" in which the C···O distance is constrained to values different from the one found in the actual transition state. Similarly, we have evaluated the change in energy which results from constraining the C···H···O angle at values other than the one found in the transition state. In all such distorted transition states, complete geometry optimizations have been carried out (except for the constraints described above). We have used these results to develop a modified MM2 force field for the calculation of intramolecular hydrogen abstractions and then evaluate the factors that influence reactivity in such systems. This has allowed us to investigate a number of issues raised by organic chemists for intramolecular hydrogen abstraction reactions such as those involved in lead tetraacetate induced formation of tetrahydrofurans from alcohols, the Barton reaction, the Hofmann–Löffler–Freytag reaction of amines, the Norrish type II reaction of excited states of ketones, and the McLafferty rearrangement of ketone radical cations. For example, why are six-membered transition states highly favored in these reactions? Is the six-membered transition states favored by enthalpy or entropy or both?[11i,16] Does the hydrogen transfer occur with a linear geometry for this reaction, and as proposed for the Hofmann–Löffler–Freytag rearrangement[11h] and for the Norrish type II process in the triplet state of ketones?[11i] These and related questions are answered for intramolecular hydrogen abstractions by alkoxy radicals in this paper.

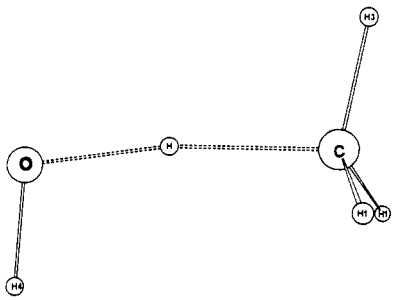

Figure 1. UHF/3-21G transition state of the $OH^{\bullet} + CH_4$ reaction.

Table I. Transition-State Geometries for the CH_4 + $OH^{\bullet}$ Reaction

	HF/3-21G	MP2/6-31G**
C···H	1.3640	1.2034
C–H	1.0778	1.0822
C–H_3	1.0780	1.0826
O···H	1.1714	1.2816
O–H_4	0.9777	0.9706
$\angle H_1$–C···H	105.29	107.55
$\angle H_3$–C···H	101.90	104.27
∠O···H···C	171.49	170.52
$\angle H_4$–O···H	102.25	98.41

Results and Discussion

Ab Initio Study of Distortion Energies of the Transition State for Hydrogen Abstraction by Hydroxyl Radical from Methane. The transition state

(8) Dorigo, A. E.; Houk, K. N. *J. Am. Chem. Soc.*, **1987**, *109*, 3698.
(9) Brun, P.; Waegell, B. In *Reactive Intermediates*; Abramowitch, R. A., Ed.; Plenum: New York, 1983; Vol. 3, p 378 ff.
(10) (a) Hortman, A. G.; Youngstrom, R. E. *J. Org Chem.* **1969**, *34*, 3392. (b) Gibson, T. W.; Erman, F. W. *J. Am. Chem. Soc.* **1969**, *91*, 4771.
(11) (a) Barton, D. H. R.; Beaton, J. M.; Geller, L. E.; Pechet, M. M. *J. Am. Chem. Soc.* **1960**, *82*, 2640. (b) Barton, D. H. R.; Beaton, J. M. *Ibid.* **1960**, *82*, 2641. (c) Barton, D. H. R.; Beaton, J. M.; Geller, L. E.; Pechet, M. M. *Ibid.* **1961**, *83*, 407. (d) Barton, D. H. R.; Beaton, J. M. *Ibid.* **1961**, *83*, 4083. (e) Nussbaum, A. L.; Carlon, F. E.; Oliveto, E. P.; Townley, E.; Kabasakalian, P.; Barton, D. H. R. *Ibid.* **1960**, *82*, 2973. (f) Heusler, J.; Kalvoda, J.; Wieland, P.; Anner, G.; Wettstein, A. *Helv. Chim. Acta* **1963**, *46*, 352. (g) Heusler, K.; Kalvoda, J. *Angew. Chem., Int. Ed. Engl.* **1964**, *3*, 525 and references cited therein. Related intramolecular hydrogen abstractions are well-known in the Hoffman–Löffler–Freytag reaction: (h) Corey, E. J.; Hertler, W. R. *J. Am. Chem. Soc.* **1960**, *82*, 1657 and references therein. (i) the Norrish type II reaction: Wagner, P. J.; Kelso, P. A.; Zepp, R. G. *J. Am. Chem. Soc.* **1972**, *94*, 7480. Wagner, P. J.; Kelso, P. A.; Kemppainen, A. E.; Zepp, R. G. *J. Am. Chem. Soc.* **1972**, *94*, 7500. (j) Scheffer, J. R., submitted for publication. The McLafferty rearrangement: (k) Djerassi, C. *Pure, Appl. Chem.* **1964**, *9*, 159 and references cited therein.
(12) Whiteside, R. A.; Binkley, J. S.; Krishnan, R.; DeFrees, D. J.; Schlegel, H. B.; Pople, J. A. Carnegie-Mellon Quantum Chemistry Archive, Carnegie-Mellon University, Pittsburgh, PA.
(13) 3-21G: Binkley, J. S.; Pople, J. A.; Hehre, W. J. *J. Am. Chem. Soc.* **1980**, *102*, 939. 6-31G**: Hariharan, P. C.; Pople, J. A. *Theor. Chim. Acta* **1973**, *28*, 213.
(14) Møller, C.; Plesset, M. S. *Phys. Rev.* **1934**, *46*, 618. Pople, J. A.; Binkley, J. S.; Seeger, R. *Int. J. Quantum Chem.* **1976**, *S10*, 1.
(15) Binkley, J. S.; Frisch, M.; Krishnan, R.; DeFrees, D.; Schlegel, H. B.; Whiteside, R.; Fluder, E.; Seeger, R.; Pople, J. A. Carnegie-Mellon University, Pittsburgh, PA.
(16) Meador, M. A.; Wagner, P. J. *J. Am. Chem. Soc.* **1983**, *105*, 4484.

calculated by using the 3-21G basis set is shown in Figure 1. A comparison between the geometry of this transition state and the one calculated by Pople at the MP2/6-31G** level is shown in Table I. The better calculation predicts a considerably earlier transition state, with the breaking CH bond length 0.16 Å shorter and the forming OH bond length 0.11 Å longer than at the 3-21G level. However, the C···O distance is very similar in the two cases (3-21G, 2.53 Å; MP2/6-31G**, 2.48 Å). Calculations with the 3-21G basis set overestimate the activation energy by about 25 kcal/mol (calculated, 29.3 kcal/mol; experimental, 5 kcal/mol[17,18]). Moreover, the reaction is predicted to be endothermic (ΔE = +11.6 kcal/mol), contrary to experimental evidence;[17] this is reflected in the incorrect "lateness" of the transition state. The MP2/6-31G** activation energy is 7.1 kcal/mol, and the reaction energy is −10.1 kcal/mol. The remaining geometry differences are minor and consistent with the usual distances found in ground-state calculations with these two basis sets.

Next, a number of distorted transition states were located, each having either the C···O distance or the C···H···O angle constrained to a value differing from the one found in the actual transition state. Changing the C···O distance brought about a significant variation in the C···H and O···H lengths but not in the C···H···O angle, even though this was not constrained at a fixed value. This means that the resulting energy change was caused mainly by the distortion of the breaking and forming bond lengths. When the angle was constrained at different values, there were only modest changes in the C···H, O···H, and C···O distances. We can conclude that even in these cases, the increase in energy was largely due to the distortion from the ideal C···H···O angle and not to the small concurrent bond length changes.

The calculated activation energy of this and other hydrogen atom transfers[19,20] depends on the theoretical level of the calculation, with correlation energy corrections necessary for reasonable activation energies. The UHF/3-21G prediction of activation energies is very poor, and it was therefore necessary to verify whether our 3-21G calculations of the distorted transition states would give reasonable relative activation energies for the distorted quasi transition states. The energies of the optimized geometries of the real and distorted transition states derived with the 3-21G basis set were recalculated at the MP2/6-31G** level. It should be noted that the minimum-energy geometry at this level has a shorter C···O distance than is found with the 3-21G basis set, while the C···H···O angle is approximately the same. The energy increment upon a given C···O distortion is somewhat higher at the MP2/6-31G** level than at the HF/3-21G level, while both calculations give very similar results for the C···H···O angle distortions. These results are summarized in Table II. Here ΔR and ΔA are the deviations from the minimum-energy values of the C···O distance and the H···C···O angle at the two levels of theory. ΔE(3-21G) represents the energy relative to the minimum-energy transition state calculated at the 3-21G level. ΔE(MP2/6-31G**//3-21G) is the energy relative to the minimum-energy transition state according to the MP2/6-31G** calculations using the 3-21G optimized geometries.

Table II. Energies (kcal/mol) of Transition-State Distortions by 3-21G and MP2/6-31G Calculations**

ΔR	ΔA	ΔE(3-21G)	ΔE(MP2/6-31G**//3-21G)
0.03		0.1	0.1
0.08		0.5	0.8
0.10		0.8	1.2
0.20		2.9	4.3
0.30		6.0	9.0
−0.05		0.2	0.3
−0.10		1.0	1.2
	5	0.05	0.06
	−5	0.05	0.05
	−10	0.3	0.4
	−15	0.6	0.7
	−20	1.4	1.5

A distortion of 0.1 Å causes an increase in the activation energy of 1.2 kcal/mol (MP2/6-31G**), which should result in a sevenfold decrease in reactivity at room temperature. For comparison, a 0.1-Å C–O stretching in methanol causes a 3.6 kcal/mol increase in energy according to HF/3-21G calculations.[21] In other words, stretching the C···O bond in the transition state is three times easier than stretching a standard C–O bond. If the deviation is equal to 0.3 Å, the calculated increase in activation energy is roughly 9.0 kcal/mol, corresponding to a decrease in reactivity by a factor of about 3×10^6. This large deceleration will ensure that in systems where the C···O distance cannot be less than 2.8 Å, other reactions, such as intermolecular hydrogen transfer, will become predominant. Intramolecular hydrogen transfer should be a very minor event, or not occur at all, in such cases. This is in agreement with the proposal by Brun and Waegell[9] and by Moriarty,[22] who proposed that such systems with C and O more than 2.8 Å apart cannot undergo this type of reaction. There are, however, several systems in which the C···O distance is higher than 2.8 Å in the minimum-energy conformer but which can assume a different conformation, bringing the reacting units in much closer proximity, at a modest expense of energy. Such systems can then undergo the reaction, sometimes in very high yield (see below).

Angular distortions have a lower but not negligible influence on the transition state stability. As shown in Table II, a 20° deviation from the ideal angle of migration destabilizes the transition state by 1 kcal/mol. This is the same change caused by a 0.1-Å distortion. By comparison, a C–O–H 20° angular distortion in methanol is accompanied by a 9.1 kcal/mol increase in energy.[21] These data are in agreement with conclusions by Menger and others that a change in the distance is more critical than a change in the angle. These calculations thus provide further evidence against the idea that the rate of a reaction should be critically dependent on small changes in the relative orientation of the reacting units.[1]

MM2 Modeling of Intramolecular Hydrogen Abstractions

We have next considered the application of these results to the study of the radical cyclization of alcohols on treatment with an oxidizing agent, usually lead tetraacetate (LTA). The reaction mechanism is shown in simplified form in Scheme I for the reaction of 1 with LTA. This is one of the systems for which it has been proposed[7,9] that the reactivity depends essentially on the distance between the alcoholic oxygen and the carbon from which the hy-

(17) Kerr, A. J. In *Free Radicals*; Kochi, J. K., Ed.; Wiley: New York, 1973; Vol. I, p 14 ff.
(18) Kabasakalian, P.; Towney, E. R. *J. Am. Chem. Soc.* **1962**, *84*, 2711.
(19) $OH^{\bullet} + H_2$: Walch, S. P.; Dunning, T. H. *J. Chem. Phys.* **1980**, *72*, 1303. See also ref 12.
(20) $H^{\bullet} + CH_4$: Morokuma, K.; Davis, R. E. *J. Am. Chem. Soc.* **1972**, *94*, 1060. See also ref 12.
(21) Dorigo, A. E.; Houk, K. N., unpublished results.
(22) Moriarty, R.; Walsh, H. G. *Tetrahedron Lett.* **1965**, 465.

Scheme I. Mechanism of the Formation of Cyclic Ethers from the Reaction of Alcohols with LTA

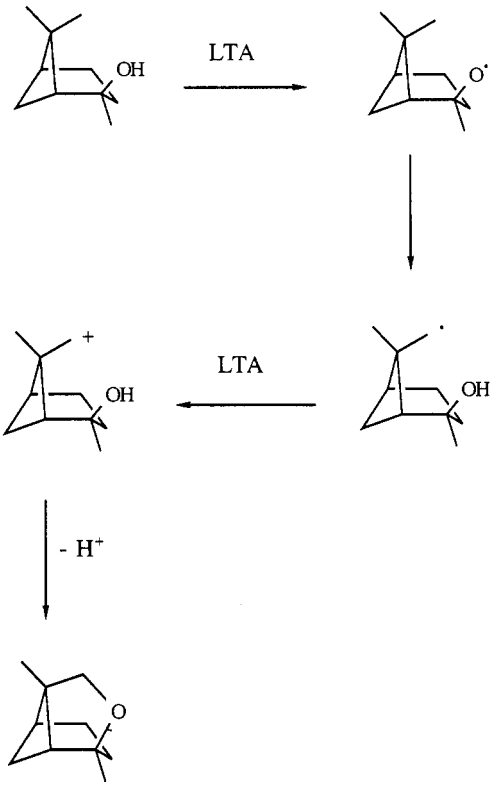

drogen atom is abstracted. The reaction involves the formation of an alkoxy radical, which can then abstract a hydrogen intramolecularly from a carbon atom (usually δ) to give an alkyl radical. The latter then cyclizes to give the ether product. An alternative mechanism involves the formation of the product directly from the alkoxy radical in one concerted step.[11g,23] In any event, the hydrogen abstraction is caused by the alkoxy radical. Figure 2 shows the structures of a number of bicyclic alcohols and the experimental yields of cyclic ether obtained upon treatment with LTA, which range from very high (alcohols 1 and 5) to zero (alcohols 2 and 4).[24]

This reaction is therefore closely related to the simple $OH^{\bullet} + CH_4$ reaction which we have investigated by ab initio techniques. Thus we should expect the transition state for the intramolecular hydrogen abstraction in this series of alcohols to have similar geometric features to the one derived from our ab initio calculations. Since systems of the size of 1–7 cannot be studied by ab initio calculations, we have devised a force field, based on Allinger's[25] MM2 program, to study these reactions.

We first investigated the structures of reactants, using standard MM2 parameters. The calculation of the geometries and strain energies of some of the starting materials had previously been performed by Brun and Waegell[26] using an early Westheimer[27] force field. They found that that the yield of cyclized product obtained by reaction with LTA was related to the calculated distance between the alcoholic oxygen and the reacting carbon atom, an underlying assumption being that the yield of this reaction is proportional to the reactivity in each case. We have repeated the calculations on alcohols 1–7 using MM2.[25] Our data, together with Waegell's and the yields of the reaction of each alcohol with LTA, are shown in Table III. Our results differ markedly from those reported by Waegell. In most cases, the carbon–oxygen distance does not vary significantly from 3.0 Å. The relationship between experimental reaction yields and calculated C···O distances in each case is discussed below.

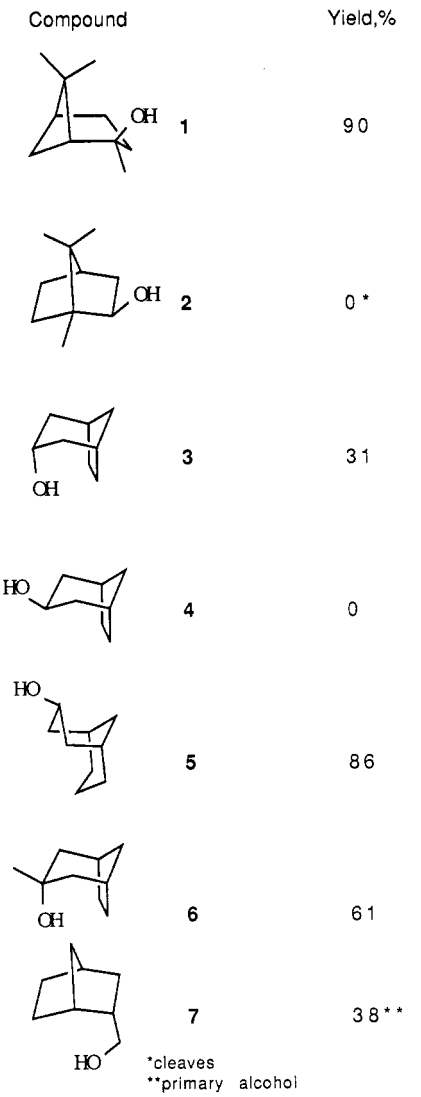

Figure 2. Structures of bicyclic alcohols 1–7 and yields of the oxidative cyclization to tricyclic ethers.

Table III. Yields of Tetrahydrofurans from LTA Oxidations of Alcohols 1–7 and C•••O Distances in 1–7

alcohol	yield, %[a]	r(C···O)	r(C···O)[c]
1	90	2.3[a]	2.96
2	0	2.8[a]	3.07
3	31	2.5[b]	3.05
4	0		4.17[d]
5	86		4.59[e]
6	61	2.4[b]	3.03
7	38		4.42

[a] Reference 9. [b] Reference 26. [c] Present study, using Allinger's MM2 force field. [d] Chair conformation; this alcohol would have to achieve a boat conformation in order to react. [e] Boat conformation; in the chair conformation the C···O distance is 3.12 Å. The calculated energy difference betweent he two conformers is 1.1 kcal/mol in favor of the boat conformer. This is in good agreement with previously reported spectroscopic data.[28]

(23) Partch, R. E. *J. Org. Chem.* **1963**, *28*, 276.
(24) Mihailovic, M. Lj.; Cekovic, Z. *Synthesis* **1970**, 209.
(25) (a) Allinger, N. L. *J. Am. Chem. Soc.* **1977**, *99*, 8127. (b) Burkert, U.; Allinger, N. L. *Molecular Mechanics*;American Chemical Society: Washington, DC, 1982.
(26) Brun, P.; Waegell, B. *Bull. Soc. Chim. Fr.* **1972**, 1825. Fournier, J.; Waegell, B. *Bull. Soc. Chim. Fr.* **1973**, 1599.
(27) Westheimer, F. H. In *Steric Effects in Organic Chemistry*; Newman, M. S., Ed.; Wiley: New York, 1956.
(28) Vegar, M. R.; Wells, R. J. *Tetrahedron Lett.* **1971**, *30*, 2847.

It appears at first that there is no correlation between our calculated C···O distances and the experimental reaction yield. However, in some cases other factors intervene which decrease or completely inhibit product formation. Thus alcohol **4**, as noted in Table III, would have to achieve a boat conformation in order to react. In the latter conformation, the C···O distance would certainly be much smaller than the one calculated for the chair form; in practice, the energy required to achieve a boat conformation is so high that the reaction is suppressed completely. In the case of **7**, the calculated C···O distance is large, and a very low yield might be expected; however, in this case rotation about the exocyclic C–C bond can bring the hydroxyl group and the reacting carbon atom at a suitable distance for hydrogen abstraction, at the expense of a modest amount of energy. Finally, **2** would be expected to be quite reactive, but gives none of the cyclic product. This is due to the fact that another reaction (β-fragmentation[23]) occurs preferentially, due to the strain in **2** and the tertiary bridgehead carbon. The other four alcohols show reactivities which are in qualitative agreement with the correlation of distance and reactivity. However, **5**, in which the C···O distance is still fairly large even in the chair conformation, is in fact very reactive experimentally and according to our calculations, described later. These results support to some extent the idea that there is some qualitative relationship between the rate of an intramolecular reaction and the distance between the reacting moieties. However, this is still a drastic approximation, since the energy required to modify this distance by a given amount can vary noticeably from one molecule to another. It is evident, for example, that a decrease in the C···O distance in alcohol **5** must not involve a large energy expenditure, since the reaction yield in this case is very high. In other words, **5** is close in energy to the transition state of the reaction, even though the C···O equilibrium distance, even in the disfavored chair conformer (ca. 3.1 Å), is considerably longer than the transition-state C···O distance calculated by ab initio methods for the model reaction between $OH^{\bullet}$ and CH_4 (ca. 2.5 Å as discussed previously).

Development of Force-Field Parameters

Force-field calculations of transition-state energies[29] present several different types of problems. The first is that the optimization algorithm used in MM2 locates an energy minimum, whereas a transition state is a maximum along the reaction coordinate. However, since the transition state calculations described before show that the partial O···H and H···C bonds in the transition state are fairly rigid, we chose to treat the transition state as an energy minimum, using the MP2/6-31G** geometry to define the unstrained O···H and C···H bond lengths and associated angles, and the distortion energies described earlier to create force constants for these new bond types. With these additions to MM2, the transition state is treated as a normal molecule, with any deviations from the ideal transition state geometry induced by other atoms resulting in an increase in energy. During the course of our work, an MM2 force field was devised by Green et al. to calculate the energies of isomeric transition states of the intramolecular hydrogen transfer in the 2-hexyloxy radical.[30] Although the parameters were developed by fitting to experimental results, the basic philosophy of treating the transition state as a minimum was also used in that work and has been used in several other studies of organic reactions, particularly by DeTar and co-workers.[29]

The MM2 force field is parameterized to reproduce quite accurately geometries and heats of formations of molecules in their ground states but not for reaction transition states. We had to develop a new set of MM2 parameters in order to calculate the steric energy of the transition states of the reactions of the compounds in our study. These parameters are based on the results of our ab initio study of the $OH^{\bullet} + CH_4$ reaction. The full parameter list is provided in the Appendix. The geometry of the transition state calculated by Pople at the MP2/6-31G** level[12] is used in defining the lengths of the C···H and O···H bonds and all angles involving either of these bonds. Note in Table I that the ab initio calculation gives two slightly different values for the H–C···H angles. In the model we use the mean of these two values for all C–C···H and H–C···H angles.

The evaluation of the force constants to be used in our MM2 model is less straightforward. In their recent molecular mechanics calculations on the transition state of the intramolecular hydrogen transfer in the 2-hexyloxy radical, Green et al.[30] used empirical parameters for the partially formed C···H and O···H bonds and for the C···H···O angle. Their model allowed only minimal motions of the C···H···O unit. According to their calculations, only a transition state in which this angle is very close to 180° (>150°) is compatible with the experimental diastereoselectivity and isotope effect observed in the reaction of deuterated substrates. In our case, bond lengths and angles are derived directly from our ab initio calculations, but the force constants cannot be obtained in the same way. In MM2, the energy is calculated as a sum of components, some of which are parameterized by force constants of different types (stretching, bending, etc.) and others which are not, like the van der Waals and dipole terms. In ab initio geometry optimizations, on the other hand, there is no such partitioning; all energy "components" are implicitly taken into account in the optimization. The resulting Hessian thus carries a different information than the MM2 matrix, which does not account for van der Waals interactions or dipole energies. Thus, one cannot simply take the ab initio force constants—or scaled force constants—and use them in the MM2 calculations.

The MM2 force constants for the forming bonds were set so as to reproduce the energy variations obtained on the distorted transition states (as defined in Table II) at the MP2/6-31G**//3-21G level. As shown in Table IV, the ab initio and MM2 relative energies of "real" and distorted transition states match very well for $k_{C\cdots H}$ = 3.9 mdyn Å^{-1}, $k_{O\cdots H}$ = 3.3 mdyn Å^{-1}, and $k_{O\cdots H\cdots C}$ = 0.130 mdyn Å deg^{-2}. These energies in MM2 are found to be dependent on the sum of the C···H and O···H force constants, rather than the individual values of each, over a wide range. The best fit with the ab initio results is obtained for $k_{C\cdots H} + k_{O\cdots H}$ = 7.2 mdyn Å^{-1}. The values assigned to $k_{C\cdots H}$ and $k_{O\cdots H}$ reflect that in the early transition state the C···H bond has a higher "bond order" than the O···H bond. For comparison, the MM2 force constant for normal C–H and O–H bonds is 4.6 mdyn Å^{-1}, respectively. The force constant for the angle O···H···C is roughly one-third of that for a standard O–C–O angle. This value is much smaller

(29) Others have previously used force fields to evaluate steric effects and model transition states in organic reactions. See, for example: DeTar, D. F.; McMullen, D. F.; Luthra, N. P. *J. Am. Chem. Soc.* **1978**, *100*, 2484. DeTar, D. F. *Biochemistry* **1981**, *20*, 1730. DeTar, D.; Luthra, N. P. *J. Am. Chem. Soc.* **1980**, *102*, 4505 and references therein.

(30) Green, M. M.; Boyle, B. A.; Vairamani, M.; Mukhopadhyay, T.; Saunders, W. H., Jr.; Bowen, P.; Allinger, N. L. *J. Am. Chem. Soc.* **1986**, *108*, 2381.

Table IV. Comparison of the Relative Energies of Distorted Transition States Derived from MP2/6-31G//3-21G Calculations and from the Modified (See Text) MM2 Force Field, for Different Values of the Stretching Constants $\nu_{C\cdots H}$ and $\nu_{O\cdots H}$ and the Bending Constant $\delta_{O\cdots H\cdots C}$[a]**

$\nu_{C\cdots H}$, mdyn Å^{-1}	$\nu_{O\cdots H}$, mdyn Å^{-1}	$\delta_{O\cdots H\cdots C}$, mdyn Å deg^{-2}	ΔR	ΔA	ΔE(MP2/6-31G**)	ΔE(MM2)
3.900	3.300	0.130				
			0.03		0.1	0.0
			0.1		1.2	1.2
			0.2		4.3	4.2
				−5	0.1	0.1
				−10	0.4	0.3
				−20	1.5	1.4
3.900	3.300	0.065				
			0.03		0.1	0.0
			0.1		1.2	1.2
			0.2		4.3	4.2
				−5	0.1	0.0
				−10	0.4	0.2
				−20	1.5	0.7
3.900	3.300	0.260				
			0.03		0.1	0.0
			0.1		1.2	1.2
			0.2		4.3	4.2
				−5	0.1	0.1
				−10	0.4	0.6
				−20	1.5	2.4
1.950	1.650	0.130				
			0.03		0.1	0.0
			0.1		1.2	0.6
			0.2		4.3	2.1
				−5	0.1	0.1
				−10	0.4	0.3
				−20	1.5	1.2
1.950	1.650	0.260				
			0.03		0.1	0.0
			0.1		1.2	0.6
			0.2		4.3	2.1
				−5	0.1	0.2
				−10	0.4	0.6
				−20	1.5	2.4
1.950	1.650	0.065				
			0.03		0.1	0.0
			0.1		1.2	0.6
			0.2		4.3	2.1
				−5	0.1	0.0
				−10	0.4	0.2
				−20	1.5	0.6

[a] ΔR is the deviation from the minimum-energy (at the MP2/6-31G** level) C···O distance and ΔA the deviation from the minimum-energy C···H···O angle.

than that used by Green et al.[30] (0.62–1.00 mdyn Å deg^{-2}).

Other force constants were determined as follows.

(1) Torsional constants for rotations about both the breaking and the forming bonds are set to zero. We feel justified in doing so, since the ab initio study shows that the frequency of torsion for such rotation is very low (38 cm^{-1}).

(2) Force constants for bending involving either (but not both) of the two partial bonds to hydrogen are expected to lie in between those involving standard bonds and that for the C···H···O angle bending. Thus, constants involving the H–O···H, H–C···H, and C–C···H angles were assigned values equal to half of the corresponding standard MM2 constants. We then verified that the strain energy of the real and distorted (as defined previously) transition states did not vary appreciably over a wide range of values for these bending constants, being essentially dependent only on the C···H and O···H stretching constants and the C···H···O bending constants. This is quite natural since all other modes are not crucial to the course of the reaction. All bond angles other than ∠C···H···O are in fact very similar in the real and in the distorted transition states. It follows that the energy of the system is essentially unaffected by tightening the force constants for distorting these angles.

(3) All other bonds, angles, and torsional constants and all nonbonded repulsions are given standard MM2 values.

This MM2 model, using parameters derived from ab initio theoretical analysis, allows us to estimate the energies of transition states of hydrogen abstraction reactions. The relative strain energy of the transition state and the corresponding alkoxy radical (ΔE) should be proportional to the activation energy of the hydrogen abstraction reaction. If the overall rate of product tetrahydrofuran formation is assumed to depend on the rate of intramolecular hydrogen abstraction versus the rate of background (e.g., intermolecular) reactions, then the ΔE should be proportional to product yields.

Our transition-state force field should be applicable to intramolecular hydrogen abstractions from secondary alkyl groups. However, a direct comparison might not be possible of a reaction which gives a primary alkyl radical, such as **1**, with one that gives a secondary, more stable radical, such as **3**. Experimentally, hydrogen abstraction by the hydroxy radical from the CH_2 group in propane has a lower activation energy than the reaction with ethane.[17] Our force field does not account for the greater stability of a more substituted radical. Thus, our calculated values of ΔE might require different "correction factors" according to the case.

Table V. Model of Hydrogen Abstraction from Ethane and Propane[a]

reactants	E_{sm}	E_{ts}	ΔE	E_a[19]
$OH^{\bullet} + C_2H_6$	0.8	0.4	−0.4	1.6
$OH^{\bullet} + C_3H_8$	1.5	0.5	−1.0	0.9

[a] Steric energies of starting materials (E_{sm}) and transition states (E_{ts}) and calculated ($\Delta E = E_{ts} - E_{sm}$) and experimental ($E_a$) activation energies are given in kcal/mol.

In order to test the behavior of our model in this respect, we optimized the transition states of the reactions between hydroxy radical and ethane and between hydroxy radical and a secondary hydrogen of propane. The steric energy of the transition state in each case (E_{ts} in Table V) is then compared to that of the starting materials, E_{sm}. The difference $E_{ts} - E_{sm}$ is the calculated activation energy, ΔE. Our results are shown in Table V, in which we compare ΔE to the experimental activation energy $E_{a,exp}$ for the two systems. The structures of the transition states are shown in Figure 3. As the table shows, the relative strain energies from our force-field are 2 kcal/mol less than the activation energies of both processes.[17] Both experimentally and according to our model, the reaction with propane has a lower activation energy than that with ethane. Experimentally, this is presumably due, at least in part, to the incipient formation of a more stable secondary radical in the case of propane. The result of our calculation, on the other hand, can be interpreted in terms of greater relief of van der Waals interactions in the transition state of the reaction of propane. As the central C···H bond lengthens, the steric repulsion between this hydrogen and the terminal hydrogens on either end of the molecule is alleviated. Naturally, this effect is larger than it is in ethane. Thus, our force field unexpectedly, but gratifyingly, appears to be adequate for the modeling of the reactivity of methyl and methylene groups alike. Moreover, the experimental activation energy can be predicted in the general case by adding 2.0 kcal/mol to the calculated value. All values of ΔE given in the remaining part of the paper are obtained by adding this amount to the calculated activation energies.

We now return to the modeling of the reactions of alcohols 1–7. Table VI shows the calculated values of ΔE together with the corresponding reaction yields. Figure 4 shows the calculated transition state structures for **3**, which is one of the least reactive alcohols, and **5**, which is one of the highest yielding and the one having the lowest calculated value for the energy difference between transition structure and reactant. The values of C···O for the reactants are listed again for comparison. The value of ΔE is found to be negative for **1** and for **5**; we can deduce that the activation energy for these two species is very low, as is also implied by the extremely high yields of the reactions of these compounds. The estimated values of the rate constants, derived from the Arrhenius equation, are also shown in the table. The A factor is approximately 3×10^3

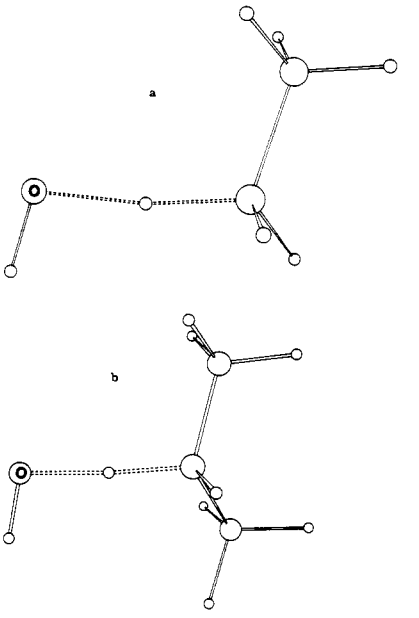

Figure 3. Structures of the MM2 transition states of the reactions between (a) $OH^{\bullet}$ and ethane and (b) $OH^{\bullet}$ and propane.

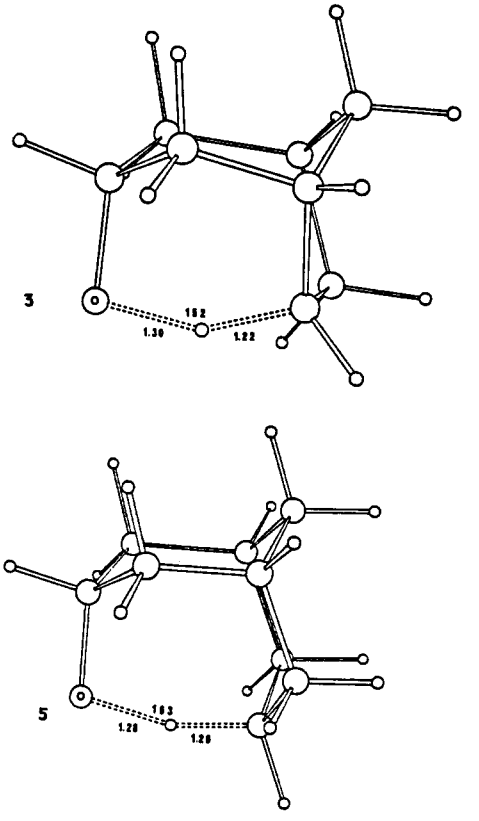

Figure 4. Structures of the transition states of the intramolecular hydrogen abstraction in alcohols **3** and **5**.

Table VI. MM2 Steric Energies of Radicals and Transition States, Predicted Activation Energies and Rate Constants, Calculated C•••O Distances in Radicals and Transition States, and Experimental Reaction Yields for Alcohols 1–7

alcohol	E_{rad}	E_{ts}	ΔE[a]	k	$r(C\cdots O_{rad})$	$r(C\cdots O_{ts})$	yield, %
1	58.4	56.3	−0.1	3.0×10^{11}	2.96	2.43	90
2	31.4	32.4	2.9	2.4×10^{9}	3.07	2.44	0
3	20.9	24.3	5.4	3.6×10^{7}	3.05	2.44	31
4	20.1	28.9	10.8	4.5×10^{3}	4.17	2.40	0
5	20.7	16.8	1.1[b]	3.0×10^{11}	4.59	2.45	86
6	21.3	24.3	5.0	7.2×10^{7}	3.02	2.43	61
7	25.5	27.3	3.8	5.4×10^{8}	3.53	2.44	38

[a] $E_{ts} - E_{rad} + 2.0$ kcal/mol. [b] See text.

L/mol·s for intermolecular reactions between $CH_3O^•$ and alkanes.[17] For intramolecular reactions we estimate that the A value is 3×10^{11} s^{-1}. The restriction of translational and rotational motions necessary in intermolecular reactions makes these approximately 10^8 slower than the corresponding intramolecular reactions.[31] The limiting value of the rate constant is then expected to be equal to 3×10^{11} s^{-1} for those compounds having very low or negative calculated ativation energies. There is good qualitative agreement between the predicted reactivity and the yields obtained, which are high for alcohols **1** and **5**, moderate for **3**, **6**, and **7**, and zero for **4**. The only exception to the general trend is alcohol **2**, which we predict to be quite reactive but which does not give any cyclized product. However, this result is most likely due to the fact that this substrate undergoes preferentially a β-fragmentation reaction,[23] as discussed previously. The calculated activation energy for the hydrogen atom transfer in **5** is −1.7 kcal/mol, so that the rate-determining step is the conversion from the boat to the chair conformer of **5**. The lower limit for the activation energy of this process is given by the difference in the stability of the two conformers, i.e., 1.1 kcal/mol (see Table III).

This MM2 model reproduces the experimental trends observed for this reaction; the general concept which we have followed can be applied to other cases as well. The main features of the calculated transition states are also of interest. The C···O distance in all cases is equal to or very close to 2.45 Å, which is essentially equal to the ab initio calculated C···O distance (2.47 Å). The C···H···O angle, on the other hand, can vary significantly from the value determined in the ab initio study (171°). This follows from the fact that the bending constant is lower than the C···H and C···O stretching constants and also lower than the other bending constants (see Appendix). The deviation from the ab initio value ranges from a minimum of 8° for alcohol **5** (the most reactive) to a maximum of 26° for alcohol **4** (the least reactive). There is no well-defined relationship between reactivity and angular distortion, however, since for all other substrates the deviation is about 20°. Rather, it is a combination of several factors, particularly torsional interactions and bending strain, that is responsible for the greater or smaller reactivity of the different compounds. For an optimal C···O transition state distance to be reached, strain has to be introduced which will vary from one compound to another; hence the differences in reactivity.

The transition state in this series of compounds is six-membered, with the exception of **5**, in which the geometry is set up perfectly for hydrogen abstraction via a seven-membered transition state. In general, the six-membered transition state resembles a flattened chair, with four coplanar atoms and the remaining two (the migrating hydrogen and the carbon atom opposite) above and below the plane, respectively. In fact, the hydrogen atom is only slightly out-of-plane, the C···H···O angle being generally close to 180° (>150°). Thus, the geometry can alternatively be regarded as an "envelope", like in cyclopentane, with an elongated "bond" made up of the C···H···O atoms (C···O = 2.5 Å). Other transition-state geometries are higher in energy but become accessible when the chair disposition cannot be achieved due to the rigidity of the system. This is the case for compounds **3** and **6**, in which the hydrogen migration takes place via a distorted boatlike transition state. However, this does not result in a high calculated activation energy. The predicted reactivity is in line with the experimental yields, which are moderate to good for the two species. In general, a distorted boatlike transition state becomes favored whenever a chairlike conformation can be achieved only by introducing severe strain in the framework of the molecule, as would be necessary for **3** and **6**. This point is also illustrated in two cases in the next section.

Scheme II. Mechanism of the Formation of Oximes by Photolysis of Alkyl Nitrites (Barton Reaction)

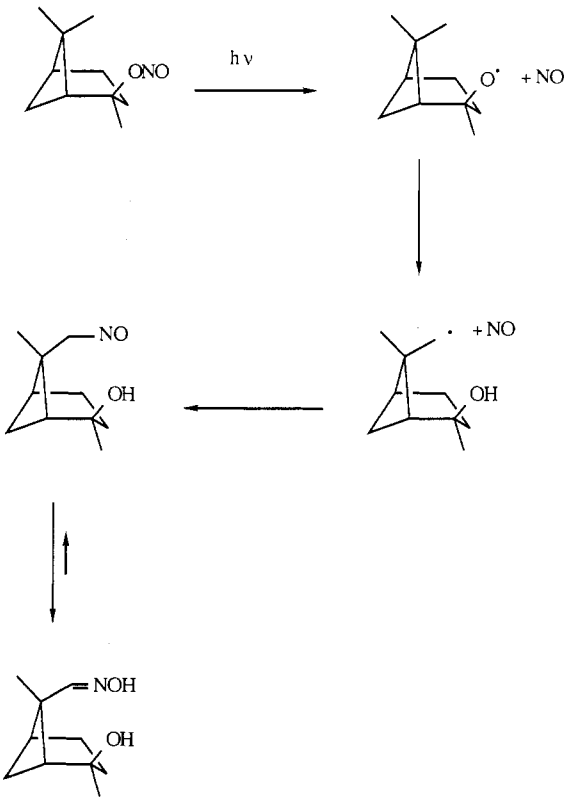

Modeling of the Barton Reaction in Steroids

The migration of hydrogen from a carbon center to an oxygen atom permits the functionalization of the carbon atom via the newly formed radical. The application of the reaction to steroid systems was introduced by Barton,[11a,b] providing a versatile and important means of introducing functionalities on angular methyl groups on the steroidal backbone. Typically, Barton's starting materials were alkyl nitrites, and the products of photolysis were the oximes derived from migration of the NO• radical. A simplified illustration of the reaction mechanism is given in Scheme II. Although the products are different from the ethers obtained from LTA oxidation, the two reactions are mechanistically very similar, the key step being hydrogen transfer in both. Accordingly, our force field can be used to model the behavior of these systems under Barton reaction conditions.

Steroids **8**–**14** (Figure 5) are among the compounds which have been reported to undergo hydrogen abstraction from alkoxy radicals.[11a-f] All the experimental yields refer to the nitrite photolysis reaction, with the exception of that for **14**, for which we give the yield of ether upon reaction of the alcohol with LTA. We have modeled the transition states for the reactions of these compounds using the same force field that we used for the bicyclic alcohols. We have replaced the side chains present in steroids **8**–**11** with hydrogen atoms in those cases where they are remote from the reacting sites. In Figure 5, the actual side chains which

(31) Jencks, W. P.; Page, M. I. *Biochem. Biophys. Res. Commun.* **1970**, *57*, 887. Page, M. I.; Jencks, W. P. *Proc. Nat. Acad. Sci. U.S.A.* **1971**, *68*, 1678. Page, M. I. *Angew. Chem., Int. Ed. Engl.* **1977**, *16*, 449.

Table VII. Steric Energies of Radicals and Transition States, Predicted Activation Energies and Rate Constants, C•••O Distances in Radicals and Transition States, and Experimental Reaction Yields for Steroids 8–14

steroid	E_{rad}	E_{ts}	ΔE	k	C···O$_{rad}$	C···O$_{ts}$	yield, %
8	43.7	47.9	6.2	1.0×10^7	3.40	2.44	34
9	44.0	45.1	3.1	1.7×10^9	2.99	2.45	47
10	41.3	41.9; 42.3	2.6; 3.0	$3.9\ (2.0) \times 10^9$	2.97; 2.87	2.44; 2.44	40; 45
11	43.8	47.3	5.5	3.0×10^7	4.34	2.44	18
12	40.6	43.8	5.2	5.1×10^7	3.41	2.45	15
13	40.3	42.2	3.9	4.5×10^8	4.32	2.44	60
14	45.8	45.1	1.3	3.3×10^{10}	3.20	2.46	90

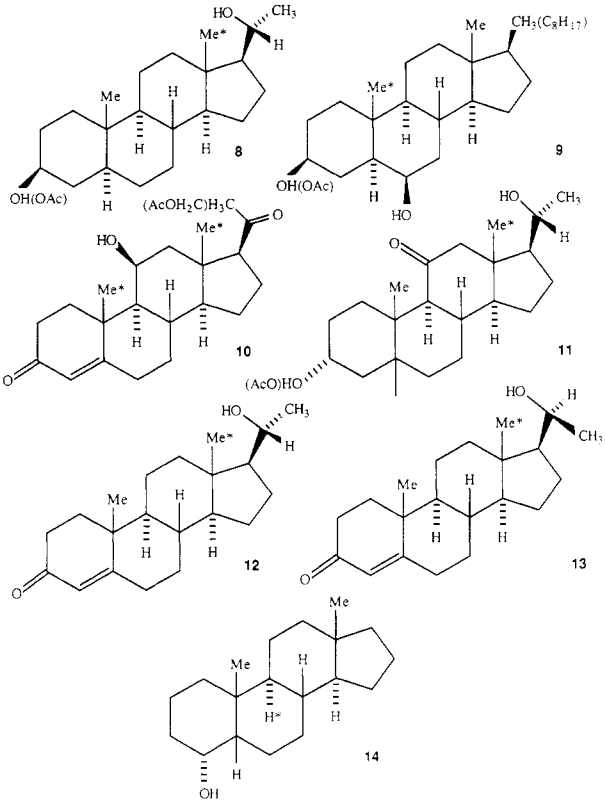

Figure 5. Structures of steroids 8–14.

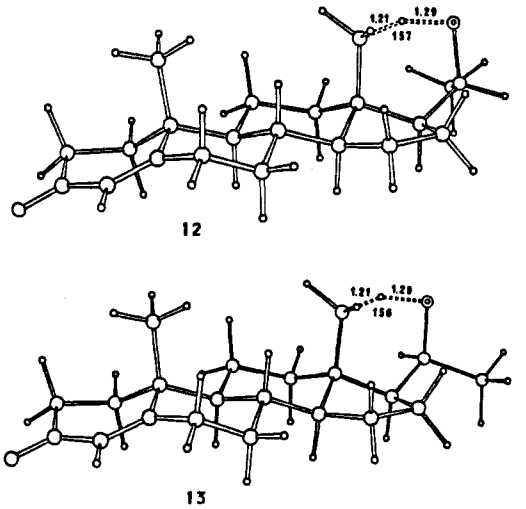

Figure 6. Structures of the transition states of the intramolecular hydrogen abstraction in steroids 12 and 13.

are present in these molecules are shown in parentheses. This permits calculations uncomplicated by the analysis of side-chain conformations. The results of our calculations and the experimental yields are described in Table VII. The calculated transition state structures for steroids 12 and 13 are shown in Figure 6 as representative cases. The reaction products for 8–13 are usually the oximes, but in some cases other products derived from the carbon radical are also found. In such cases the yield given in Table VII represents the sum of the yields of the oxime and the other products obtained. In the table, the C···O distance in the starting material is also given. There are two sets of values for compound 10 since two methyl groups can react with the alkoxy radical.

Once again, the agreement between calculated and experimental results is good. It is noteworthy that the model predicts correctly the higher reactivity of 20α alcohols over the β epimers[11e]—compounds 13 and 12, respectively. The prediction of approximately equal reactivities of the C-19 and C-18 positions in compound 10 is also reflected in the roughly equal yields of products derived from the two radicals. Most of the features of the transition state geometries are the same as discussed for alcohols 1–7. In the steroids, hydrogen migration occurs via a flattened chairlike conformation in all the transition states which are shown in Figure 6. Interestingly, for compounds 8 and 11 we have also found an alternative, boatlike transition state in each case. Figure 7 shows the chair- and boatlike transition states which are possible for the reactions of 8 (8 and 8a, respectively) and 11 (11 and 11a). Indeed, the "chair" and "boat" transition states really resemble two different forms of envelope five-membered rings. The importance of such a formulation is described in more detail in the next section. According to our calculations, the chair transition state is favored in both cases but only by 0.4 kcal/mol for 8 and by 0.2 kcal/mol for 11. This is because in the chairlike transition states (8 and 11 in Figure 7), the CH_3 group on C-21 is driven into close proximity of the hydrogen atoms on C-11. This interaction is relieved when the "boat" transition-state geometry is assumed (8a and 11a). Both compounds might have two alternative reaction pathways available, leading to a lowering of the activation energy estimated from the difference in steric energies. This effect would account for the discrepancy between the rather high activation energy calculated for 8 and the fair yield of product obtained from the reaction.

Acyclic Systems

The cyclization of acyclic aliphatic alcohols under various conditions (LTA, LTA + I_2, nitrite photolysis) invariably yields tetrahydrofurans as the major or only cyclic products.[17,32,33] Only the formation of tetrahydropyrans is sometimes competitive.[33,34] This shows that the preference for a six-membered transition state is general and not confined to those cyclic systems where the selectivity might derive from the rigidity of the skeleton. These results have been explained on the basis of favorable "through-bond" interactions stabilizing the six-membered transition state.[35] As described in more detail below, the

(32) Partch, R. E. *J. Org. Chem.* **1965**, *30*, 2498.
(33) Walling, C.; Padwa, A. *J. Am. Chem. Soc.* **1963**, *85*, 1593.
(34) Cope, A. C.; Bly, R. S.; Martin, M. M.; Petterson, R. C. *J. Am. Chem. Soc.* **1965**, *87*, 3111.

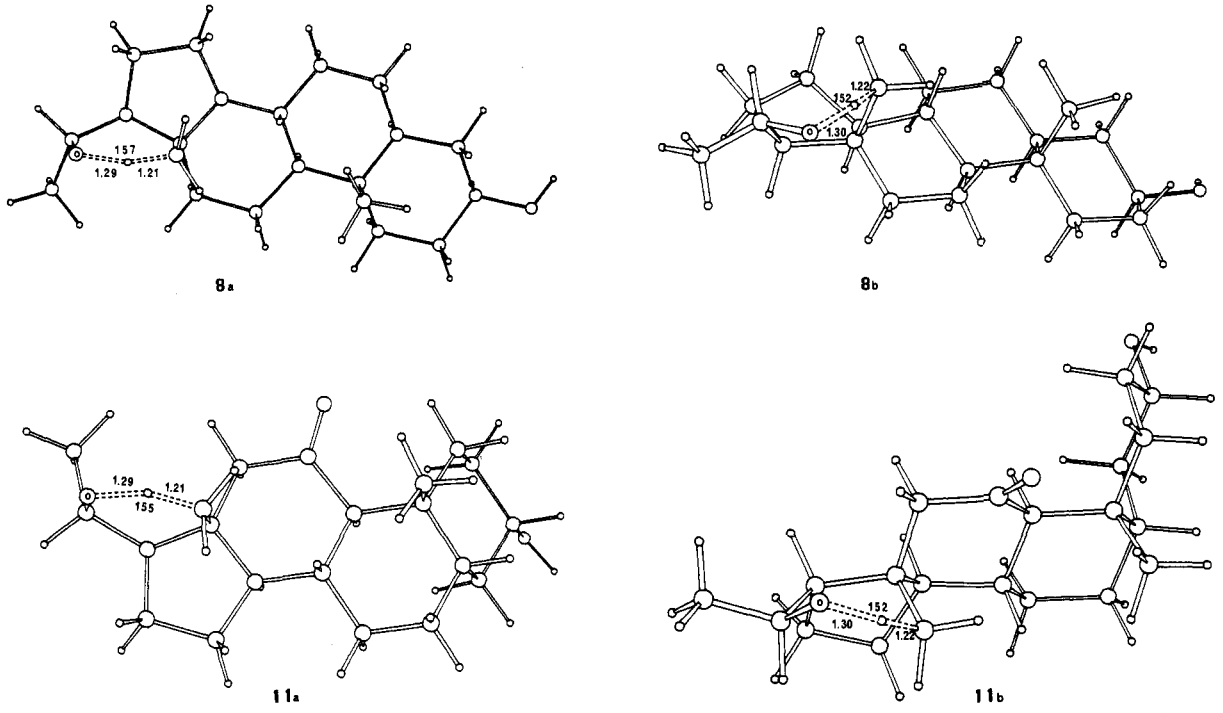

Figure 7. Structures of the transition states of the intramolecular hydrogen abstractions in steroids 8 and 11: **8a**, chair form transition state of 8; **8b**; boat form transition state of 8; **11a**, chair form transition state of 11; **11b**, boat form transition state of 11.

Table VIII. Energies of the Radicals and Transition States, and Activation Parameters[a]

	total energy, au		E_{rel}, kcal/mol					$\Delta G^{\ddagger}$		
radical[a]	UHF/3-21G	MP2/6-31G*	UHF/3-21G	MP2/6-31G*	$\Delta H^{\ddagger}$	S, eu	$\Delta S^{\ddagger}$	at 300 K	at 200 K	at 80 K
butoxy										
reactant	−230.25690	−232.18555	0.0	0.0		82.5				
TS	−230.20173	−232.16181	34.6	14.9	11.0	78.9	−3.6	12.1	11.7	11.3
pentoxy										
reactant	−269.07603	−271.35104	0.0	0.0		92.0				
TS	−269.02185	−271.32859	34.0	14.1	10.1	80.1	−11.9	13.7	12.5	11.1

[a] Enthalpies were calculated from MP2 energies by correcting for zero-point energies and for the RT and C_pT terms (T = 298 K). Entropies were derived from the calculated geometries and harmonic vibrational frequencies. Correction factors of R ln 9 and R ln 27 are added to the calculated entropies of the butoxy and pentoxy radicals, respectively, to account for the number of conformers available. Correction factor of R ln 2 is added to the entropy of each transition state, to account for the existence of an enantiomeric transition state. An additional factor of 4.4 eu is added to the six-membered transition state to account for its low-frequency ring-puckering vibration (pseudorotation).[37] [b] TS = transition state.

force-field model predicted that the seven-membered transition state was 0.8 kcal/mol lower in energy than the six-membered. This surprising result led us to investigate these same reactions at the ab initio level.[8] These results will be described first.

The structures of the butoxy and pentoxy radical were optimized at the UHF/3-21G level. Single-point energy calculations were carried out on the pentoxy radical at the MP2/6-31G* level. The gauche conformation of the O–C–C–C atoms was found to be 0.4 kcal/mol (0.7 kcal/mol by HF/3-21G) lower in energy than the anti conformer. For the butoxy radical, the gauche conformation was calculated (3-21G) to be preferred by 0.7 kcal/mol. The radicals therefore prefer the gauche conformation, like the corresponding alcohols. The structures of the gauche conformers are shown in Figure 8.

Transition states for the δ-hydrogen abstraction (six-membered transition structure) in the butoxy radical and for ϵ-hydrogen abstraction (seven-membered transition structure) in the pentoxy radical were located at the UHF/3-21G level. Figure 9 shows the structures of the six- and seven-membered transition structures with details of the geometry of hydrogen transfer. Calculation of the

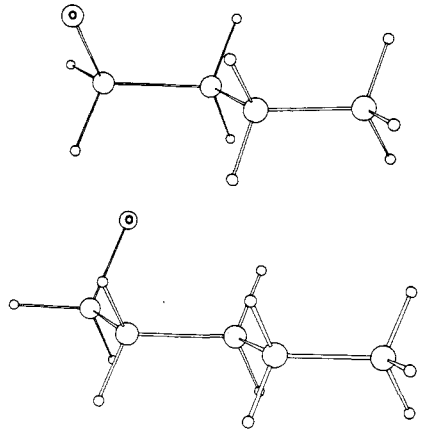

Figure 8. HF/3-21G structures of the gauche conformations of the n-butoxy (top) and n-pentoxy radicals (bottom).

harmonic vibrational frequencies showed that both are authentic transition structures having only one imaginary frequency, corresponding to hydrogen atom motion from carbon to oxygen or vice versa. Activation enthalpies for both reactions were calculated as a sum of the differences in electronic and thermal energies between starting materials and transition structures. The activation enthalpy

(35) Verhoeven, J. W.; Pasman, P. *Tetrahedron* **1981**, *37*, 943.

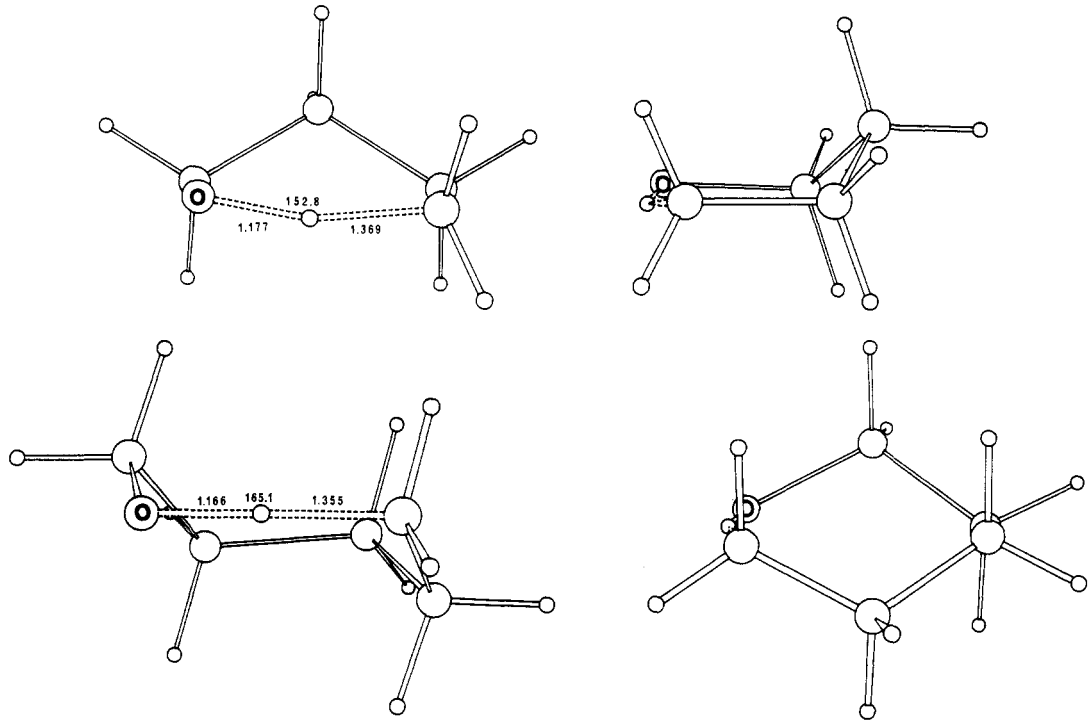

Figure 9. HF/3-21G transition structures of the intramolecular hydrogen abstraction in the *n*-butoxy and *n*-pentoxy radicals.

for the conversion of the butoxy radical to the 4-hydroxybutyl radical, via a six-membered transition structure, was calculated to be 0.7 kcal/mol higher than that for the reaction of the pentoxy radical to give the 5-hydroxypentyl radical via a seven-membered transition structure. Table VIII gives a summary of the total and *relative* energies of the species involved in the two processes.

The six-membered transition structure resembles a five-membered ring of heavy (non-hydrogen) atoms, having an envelope shape like that of cyclopentane, but with a long C–O bond. The seven-membered ring has a "chair" form like that of chair cyclohexane but again with one long bond. The O···H···C angle is slightly distorted from linearity in the seven-membered transition structure (∠O···H···C = 165.1°), and distorted to a larger extent in the six-membered transition structure (∠O···H···C = 152.8°). The C···H and O···H bond lengths, on the other hand, are similar in the two cases and very close to the bond lengths in the transition structure for the reaction between methane and the hydroxyl radical.

These results indicate that the preference for δ-hydrogen abstraction does not originate from a higher stabilization of the six-membered cyclic array. Our calculations predict instead that there is a significantly higher entropy of activation involved in the hydrogen atom transfer in the butoxy radical than in the pentoxy radical. The entropies of the reactants and transition states were computed from the calculated geometries and frequencies at the 3-21G level. The entropies of the starting radicals can also be estimated from Benson's group equivalents.[36] In either case, the entropy of the favored gauche conformation of the radical is corrected for the contribution from all other conformations in the molecule. Both methods give similar results. As shown in Table VIII, the entropies of activation are calculated to be −5.6 (−5.0) eu for the six-membered abstraction transition structure and −13.8 (−13.1) eu for the seven-membered transition structure. The difference in entropies of activation is therefore 8.2–8.3 eu corresponding to 2.5 kcal/mol at room temperature. This is very close to the 9.1 eu more favorable entropy change for conversion of pentane to cyclopentane as compared to conversion of hexane to cyclohexane.[38] Thus, we estimate that the free energy of activation is 1.8 kcal/mol lower for the six-membered transition state than for the seven-membered at room temperature. At lower temperature, the entropy term $T\Delta S$ decreases, and we predict that the seven-membered ϵ-abstraction transition state will become favored at about −190 °C and below. Our conclusions are also supported by the observations by Lefort and coworkers that the similar preference for intramolecular δ-hydrogen abstraction by carbon radicals is controlled by entropic factors, since in such systems the δ-/ϵ-hydrogen abstraction ratio varies little with temperature.[39]

Force-field modeling of the ω-hydrogen atom abstractions in the propoxy (**15**), butoxy (**16**), and pentoxy (**17**) radicals gives results in remarkable agreement with the ab initio calculations described above. Figure 10 shows the structures of the five-, six-, and seven-membered transition states involved in the reactions of **15**, **16**, and **17**, respec-

Table IX. Steric Energies of Radicals and Transition States and Calculated Activation Energies for Alcohols 15–17

radical	E_{rad}	E_{ts}	ΔE
15	2.7	10.0	9.3
16	3.4	6.7	5.3
17	3.9	6.4	4.5

(36) Benson, S. W. *Thermochemical Kinetics*, 2nd ed.; Wiley: New York, 1976.

(37) The intrinsic entropy of an acyclic hydrocarbon is obtained from that of the corresponding acyclic species by the expression[36]

$$S^0_{c,int} = S^0_{a,int} - (n-1)f$$

where n is the number of atoms in the ring. f = 4.7 eu for cyclohexane and most cyclic hydrocarbons but only 3.6 eu for cyclopentane. This low value of f in cyclopentane is due to pseudorotation.[36] Thus, the contribution of pseudorotation to the entropy of the five-membered ring is

$$[-(5-1)3.6] - [-(5-1)4.7] = 4.4 \text{ eu}$$

(38) Eliel, E. L. *Stereochemistry of Carbon Compounds*; McGraw-Hill: New York, 1962.

(39) Nedelec, J. Y.; Gruselle, M.; Triki, A.; Lefort, D. *Tetrahedron* 1977, *33*, 39.

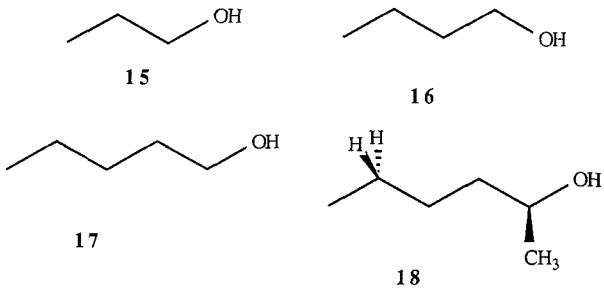

tively. As shown in Table IX, the activation energy for the five-membered transition state is by far the highest, in agreement with the lack of any experimental evidence for γ-hydrogen abstraction. The reaction via a six-membered transition state is calculated to have an 0.8 kcal/mol higher activation energy than that which occurs through a seven-membered transition state. This is the very similar to the value of $\Delta H^{\ddagger}$ derived from our MP2/6-31G**//3-21G ab initio calculations (0.7 kcal/mol).

It might seem alarming that entropy controls reactivity here, whereas our MM2 model neglects entropic considerations entirely in making predictions about rates of reactions. We clearly can only compare processes which have similar entropies of activation, using our force-field model, or we must make independent estimates of activation entropies. Presumably the entropy differences are small for the many relatively rigid polycyclic systems which we have treated here in detail.

In the recent paper by Green et al.[30] it was shown that hydrogen abstraction in the 2-hexyloxy radical (18) was not stereoselective. The ratio of rate constants for the abstraction of the α- and β-hydrogen atoms (see 18) on C-5 was found to be equal to 1.22 at 30 °C, and there was no detectable temperature dependence of this ratio, implying essentially no difference in activation energy. The authors explained the experimental results in terms of a force-field model in which the C···H···O angle was set equal to 180° and not allowed to vary. They proposed that a large (>-30°) deviation from linearity would result in H_β abstraction being appreciably favored, since the methyl group would prefer a pseudoequatorial conformation by at least 1 kcal/mol over a pseudoaxial. Our force-field and ab initio calculations predict that in the six-membered transition state this angle is 153–155°, even though the preferred C···H···O angle is 170.5°. There are two possible pathways in each case, as shown in Figure 11. The transition state for H_β abstraction (**18a**) is favored over that for H_α abstraction (**18c**) by 0.6 kcal/mol. The other two transition states, **18b** and **18d**, are 1.8 and 1.2 kcal/mol, respectively, higher in energy than **18a**. If these higher energy transition states are taken into account, the ratio of H_β to H_α abstraction is predicted to be 2.04 at 30 °C, as compared to the value of 1.22 found experimentally. Thus our model calculations are in qualitative agreement with the observed lack of stereoselectivity in the reaction.

Predictions

The good agreement between calculated activation energies and experimental yields and our belief that rate constants are being calculated properly allow us to make predictions for compounds which are unknown or whose behavior under these reaction conditions has not been studied. We first calculated the relative ease of δ- and ε-hydrogen abstraction in the 1-hexyloxy radical, which we intend to study experimentally. There are four transition states, and using the calculated activation energies of 4.6 and 5.1 for δ-abstraction and 3.8 and 4.6 for ε-abstraction, along with the same activation entropy estimates which

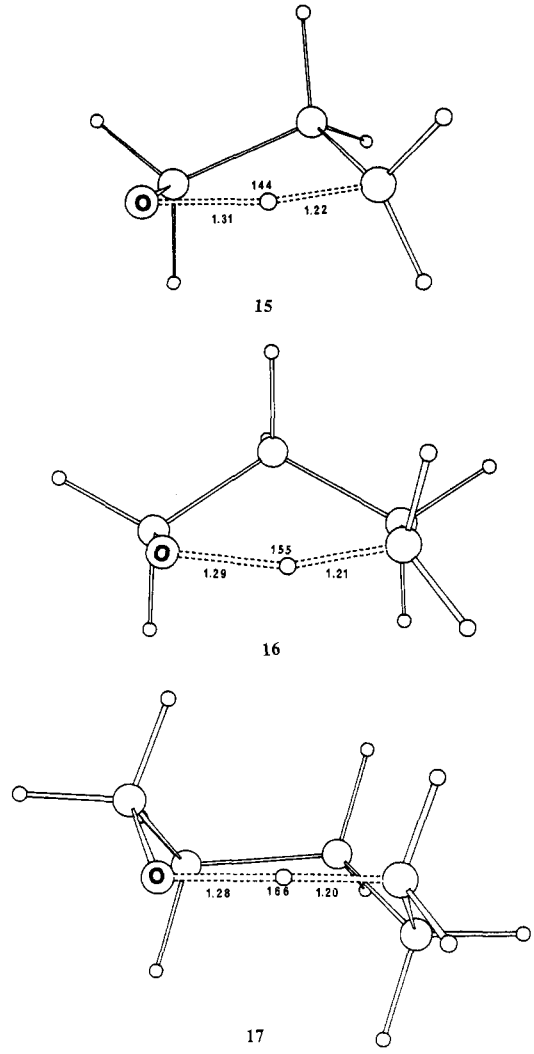

Figure 10. MM2 structures of the transition state of the intramolecular hydrogen abstractionsin the *n*-propoxy, *n*-butoxy, and *n*-pentoxy radicals.

are used earlier for δ- and ε-abstraction in butoxy and pentoxy radicals, we predict δ/ε ratios of 19.4:1 at 25 °C and 1:1 at −180 °C and a preference for ε-abstraction below −180 °C.

We also investigated the hydrogen abstraction in eight- and nine-membered transition states in the hexyloxy and heptoxy radicals. In order to calculate the transition-state energies, we first used MM2 to calculate all possible conformations of oxacycloheptane and oxacyclooctane, each having one C–O bond length fixed at 2.5 Å, which is the C···O distance in our six- and seven-membered transition states. We then used the optimized structures of the cyclic ethers as starting geometries for the transition-state calculations, inserting the migrating hydrogen atom between the carbon and oxygen atoms 2.5 Å apart, and then we optimized each transition-state conformation. This procedure ensures that all conformations of the eight- and nine-membered transition states are examined and that the lowest energy conformation is found for both systems.

The calculated C···H···O angle is very close to the ideal value of 170.5° in the most stable conformation of each transition state, being equal to 171° in the eight-membered transition structure and 170° in the nine-membered one. Three other conformations were found to be within 1 kcal/mol of the most stable eight-membered transition structure, but even for the most stable transition-state conformation the calculated activation energy is 8.0

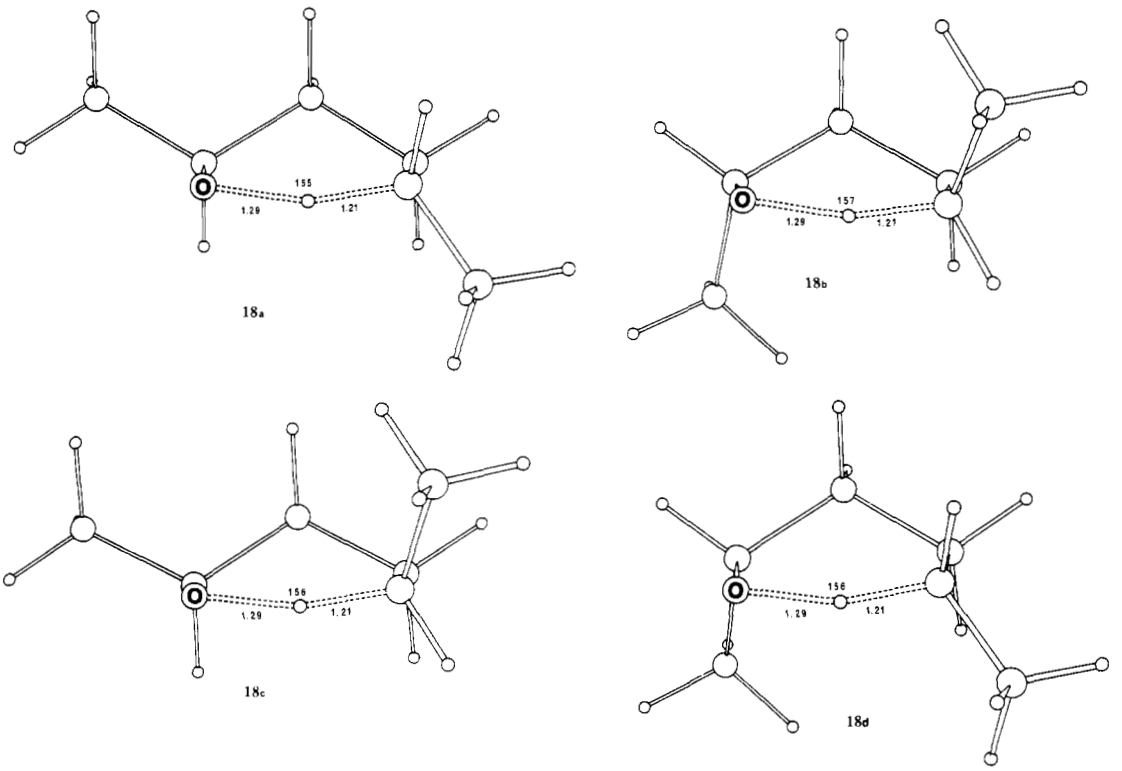

Figure 11. MM2 structures of the transition state of the intramolecular hydrogen abstraction in the 2-hexyloxy radical 18: **18a,b**, cis hydrogen abstraction; **18c,d**, trans hydrogen abstraction.

Table X. Steric Energies of Radicals and Transition States, C• • •O Distances, and Predicted Activation Energies and Rate Constants for Alcohols 19–22

alcohol	E_{rad}	E_{ts}	C···O_{rad}	C···O_{ts}	ΔE	k
19	52.0	48.0	2.73	2.37	−2.0	3.0×10^{11}
20	57.3	49.8	2.91	2.43	−5.5	3.0×10^{11}
21	60.8	57.1	2.93	2.41	−1.7	3.0×10^{11}
22	103.3	107.8	2.93	2.41	6.5	6.0×10^{6}

kcal/mol, compared to 5.3 kcal/mol for the six-membered structure and 4.5 kcal/mol for the seven-membered one. Similarly, three conformations each within 1.0 kcal/mol of the lowest energy nine-membered transition structure were found, but the lowest calculated activation energy in this case is equal to 9.1 kcal/mol. Thus, not counting entropic contributions, the geometric preference for hydrogen migration is in the order seven-membered ≫ eight-membered > nine-membered. The nine-membered transition state should have a higher entropy than the eight-membered one, owing to the low-frequency puckering motion of the former, by analogy with oxacyclooctane. This effect might compensate for the enthalpic preference for the reaction via the cyclic eight-membered structure. Both processes, however, are still much less favorable than hydrogen abstraction via a seven-membered structure. Thus, even though the eight- and nine-membered transition states can achieve a nearly ideal C···H···O arrangement, there are problems in achieving an unstrained conformation of the connecting-chain atoms.

We have also designed some polycyclic alcohols to test various qualitative notions about the relationship between proximity and reactivity. We have calculated the steric energies of starting materials (Figure 12) and transition states (Figure 13) of alcohols **19–22**, and from the ΔE values we have derived predicted rate constants for the four compounds. These results are summarized in Table X. Negative activation energies and therefore very high reactivities are predicted for three of the compounds. Of particular interest is the comparison between **19** and **22**.

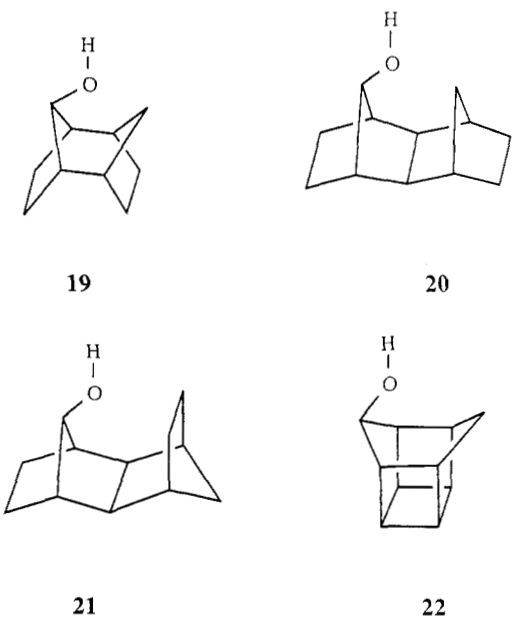

Figure 12. Structures of alcohols **19–22**.

The two compounds are very similar, except for the greater rigidity of the skeleton of **22**. The C···O distance between the reacting atoms in the starting material is also similar, and this might be expected to lead to similar reactivities. Our calculations predict instead a very high reactivity for **19** and a low one for **22**, where the formation of a cyclic

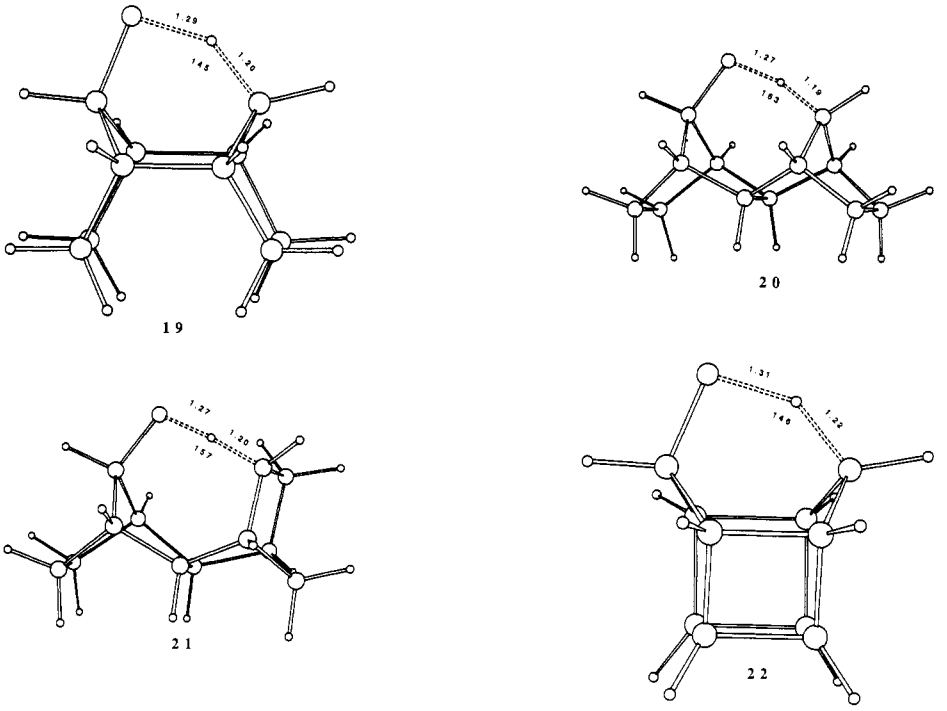

Figure 13. MM2 structures of the transition state of the intramolecular hydrogen abstractions in the alcohols **19–22**.

array in the transition state for the reaction introduces considerable strain. Exceedingly high reactivities are predicted also for **20** and **21**. The short C···O distance in the starting material and the relief of the repulsive interaction between the oxygen atom and the methylene group in the transition state are responsible for the very low activation barrier predicted for these two species.

Conclusions

Our study shows that ab initio MO theory can be combined with a force-field calculation to give relative activation energies of reactions. In such a way, the inherent rapidity of a force-field method can be combined with an ab initio theoretical analysis. The results are in agreement with the qualitative experimental data available for intramolecular hydrogen abstractions in various systems. It is also possible to make reactivity predictions on systems which have not been studied previously under these reaction conditions, or which are unknown.

Our ab initio results reaffirm that the distance between the reacting groups is not a direct measure of the reactivity. As shown by several examples in this paper, compounds in which this distance appears to be far from the ideal value of 2.5 Å are still capable of very high reactivity. On the other hand, some compounds for which the C···O distance is fairly small do not give high yields of product or are not predicted to do so. There is an intuitive qualitative relationship between the distance in the starting materials and the reactivity, but this does not result in lowering of the activation barrier if a further decrease in distance is accompanied by a substantial increase in strain in the rest of the molecule. In general, a certain energetic price must be paid in order for the reacting groups to achieve the appropriate proximity in the transition state; the rate of an intramolecular reaction depends upon how high this price is.

Although the quantum mechanical calculations predict that hydrogen transfer occurs preferentially via a nearly linear transition state, it is easy to distort to a nonlinear geometry. Indeed, all of the intramolecular hydrogen transfers are predicted to occur with distinctly nonlinear geometries, usually 150–160°. This reflects the fact that bonds to the hydrogen atom have no directional character, and it is only the repulsion between groups simultaneously bonded to hydrogen which will tend to produce a linear geometry. For the intramolecular reactions, the angles generally cluster around 155°, presumably to keep the C···O distance equal to 2.5 Å in the transition state, to maintain nearly tetrahedral C–C···H and C–O···H angles, and to keep the transferring hydrogen apart from the remainder of the molecule.

Even in intermolecular reactions of this type, the hydrogen transfer is not expected to be linear once dynamic or statistical considerations are taken into account. Just as hydrogen bonds are almost never linear in crystal structures[40] or liquid simulations,[41] even though there is a distinct energy advantage for linearity, hydrogen-transfer transition states will only rarely be linear. The energy required for the reaction to proceed via a nonlinear transition state is small, and probability favors nonlinear transition states. That is, the probability of having an exactly linear transition state is vanishingly small, while the probability for nonlinear hydrogen transfer increases as the angle decreases from 180° to 90°, simply because the number of atomic arrangements with the smaller angles is higher.[42]

What conclusion is warranted from the model about the validity of various theories of angle and proximity effects on rate? A unimolecular reaction may be 10^8 times faster than the analogous bimolecular process, if both have the same activation energy. This is due to the approximately −45 eu activation entropy which invariably occurs due to the restriction of translational and rotational entropy in a bimolecular process.[5,43] In the current example, we predict that the reaction of **14** will be 10^8 faster than the intermolecular hydrogen abstraction from ethane by an alkoxy radical. Both are prodicted to have the similar activation energies (1.3 and 1.6 kcal/mol). Other intramolecular reactions may be substantially faster or slower

(40) Narten, A. H. *J. Chem. Phys.* **1972**, *56*, 5681.
(41) Jorgensen, W. L. *J. Am. Chem. Soc.* **1981**, *103*, 341.
(42) Jorgensen, W. L., private communication.
(43) Houk, K. N.; Rondan, N. G. *J. Am. Chem. Soc.* **1984**, *106*, 4293.

than this. Reactions of **19–21** are predicted to be faster than the normal reaction of **14**, because the change in strain energy upon conversion of the alkoxy radical to the transition state is smaller than for the intermolecular reaction. These are cases where the repulsion between reactants present in the transition state of the intermolecular reaction are overcome by the binding of the reacting groups into the same molecule. There are also many examples (**3, 4, 12, 22**) predicted to go slower than the 10^8 factor. This is because the reacting groups have been "bound" too favorably relative to the transition state, or because the transition-state geometry cannot easily be achieved in the relatively rigid polycyclic framework. The primary factor of importance is that the C···O distance of about 2.5 Å must be achievable; angular factors are of less importance.

We have also found that activation entropy differences may be influential upon determining relative rates of reaction and have proposed that factors which cause the well-known anomalously favorable entropy of formation of five-membered rings operate in the hydrogen abstraction to favor the six-membered hydrogen abstraction.

Our general conclusions are essentially the same as those of Bruice,[2] Page and Jencks,[4] and Page.[5] The restriction of translational and overall rotational motions which occurs upon incorporating two functional groups into the same molecule are mainly responsible for intramolecular rate accelerations. The same effects occurring upon binding of substrates may account for the very high catalytic activity of enzymes.[4] Bruce[2] suggested that the freezing of rotations about single bonds in going from intermolecular to intramolecular reactions might be worth an additional 200-fold increase in reactivity, while Page and Jencks[4] proposed a factor of only 5 for the rate increase due to this effect. Our calculations show that when rotations about single bonds are possible, as in **7**, the experimental yield is lower than our calculation would predict. This effect is small, however, and the calculation is in good agreement with the rate factor of 5 proposed by Page and Jencks.[4] Other effects such as stringent orientational requisites are unimportant. Indeed, as shown by Page,[5] the relative rates of lactonization of several strained bicyclic acids are well reproduced by the relative energies of ring closure of analogous hydrocarbons. Thus, orbital steering[1] is a relatively small effect, and the spatiotemporal hypothesis of Menger[7] is incomplete, because it dwells on distortions in reactants, not on the ease of achieving transition-state geometries.

We are currently investigating the posibility of extensions of this force field to intramolecular hydrogen abstraction reactions involving other types of radicals, as well as ketone excited states and radical cations.

Acknowledgment. We are grateful to the National Institutes of Health and the National Science Foundation for financial support of this research and to Professors Peter J. Wagner and Sir Derek H. R. Barton for stimulating discussions.

Appendix

The following is a list of the parameters used in the force-field model of the transition states of the reaction. These parameters redefine the torsional, stretching, and bending modes involving those bonds which are being broken or formed in the reaction. For all force constants not included in the list, an "equivalence statement" has been used, whereby the three atoms involved in the transition state are treated as sp^3-hybridized carbon, alkylic hydrogen, and sp^3-hybridized oxygen atoms, respectively.

	torsional, mdyn Å		
	V_1	V_2	V_3
1p–O···H···C	0.000	0.000	0.000
H–C–C···H	0.000	0.000	0.237
H–C–O···H	0.000	0.000	0.000
C–C···H···O	0.000	0.000	0.000
C–C–C···H	0.000	0.000	0.267
H–C···H···O	0.000	0.000	0.000
C–C–O···H	0.800	0.000	0.090
C–O···H···C	0.000	0.000	0.000

	bond stretching and compression, mdyn Å^{-1}	
	k_s	l_0
C–O*	5.360	1.4465
C···H	3.300	1.2816
O···H	3.900	1.2034

	angle bending, mdyn Å deg^{-2}	
	k_θ	θ_0
1p–O···H	0.120	101.010
C–O···H	0.175	98.410
C···H···O	0.130	170.524
C–C···H	0.180	105.914
H–C···H	0.160	105.914

* Derived from ab initio calculations on alkoxy radicals (see text).

Registry No. **1**, 112574-21-7; **2**, 24393-70-2; **3**, 13387-10-5; **4**, 13387-09-2; **5**, 10036-10-9; **6**, 2565-95-9; **7**, 69831-11-4; **8**, 17182-23-9; **9**, 4470-73-9; **10**, 1173-26-8; **11**, 1053-19-6; **12**, 145-15-3; **13**, 145-14-2; **14**, 112533-34-3; **15**, 16499-18-6; **16**, 19062-98-7; **17**, 26397-35-3; **18**, 62224-40-2; **19**, 67252-91-9; **20**, 35909-27-4; **21**, 36197-17-8; **22**, 13351-16-1; H_2, 1333-74-0; HO•, 3352-57-6; CH_4, 74-82-8; C_2H_6, 74-84-0; C_3H_8, 74-98-6.